

## **THERMAL AND STRUCTURAL CHARACTERIZATION OF COKE DEPOSITION ON SPENT NiMo CATALYST USED DURING CATALYTIC UPGRADING OF HEAVY OIL**

### **ABSTRACT**

Catalyst deactivation has become a major concern in the refining industry globally. The deactivation of hydroprocessing catalyst by coke deposition reduces its useful life, the on-stream time of the process involved and the profitability of upgrading heavy oils to useful products. There are various methods used in thermal and structural characterization but for the purpose of this research journal, Thermogravimetric Analysis (TGA), Scanning Electron Microscopy (SEM), X-Ray Diffraction (XRD) and Fourier Transform Infrared (FTIR) were carried out on both fresh and spent NiMo catalyst. The TGA results of the spent catalyst samples indicates the presence of coke species with the major portion of the species being 'medium' and 'hard' coke (second and third stage). There was also no significant change in loss of weight with change in heating rate. In comparison to the fresh catalyst, the SEM micrograph of the used catalyst indicates the formation of poor porous-structure and block-shaped crystallites depicting the sintering of particles because of the higher calcination temperature. O–C–O bond stretching vibrations with an anatase morphology were observed using FTIR on the spent catalyst sample confirming the presence of the coke species while the XRD results showed the formation and nature of carbonaceous deposits on the spent catalyst's surfaces. A rutile phase with a tetragonal symmetry was detected for spent NiMo diffraction peaks, with the major phase indicating the presence of Carbon with a hexagonal phase.

**Keywords:** Catalyst, coke, NiMo, characterization, heavy oil, TGA, FTIR, SEM, XRD, hydroprocessing, catalyst deactivation.

### **1. INTRODUCTION**

Thermal cracking was previously used in upgrading heavy oil in refineries before catalytic cracking came into use as a more desirable process because of two major reasons. Catalytic cracking minimizes the yield of other products and maximizes the yield of gasoline (Sundaram, 2017). The gasoline produced by catalytic cracking is of higher quality and this is due to the various reactions that take place in the reactor during catalytic cracking. In recent years, hydroprocessing catalysts have been widely accepted and highly

preferred in the refining industry due to many reasons. One of the reasons is the result attained in the purification of different petroleum streams particularly in the catalytic upgrading of heavy oils and residues. These catalysts have also provided a very wide range of well-proven products for a wide range of hydrodesulphurization (HDS) and hydrodenitrogenation (HDN) duties. Catalysts usually used in residue hydrotreating processing consists of Molybdenum (Mo) and promoter Nickel (Ni) or Cobalt (Co) on alumina support to increase the removal of various unwanted impurities such as Nitrogen, Sulphur and metals as a result of hydrodenitrogenation, hydrodesulphurization and hydrodemetallization reactions (Zahran et al., 2020).

Catalysts are mainly used to enhance the efficiency of catalytic cracking and maximize the removal and reduction of polyaromatic content by breaking heavier hydrocarbons with higher boiling points to short-chain hydrocarbons with lower boiling points that can even be further processed in other units within the refinery (Ihediwa, 2021). In the catalytic upgrading of heavy oils, NiMo catalyst stands out as a result of its high desulphurization activity for reducing polyaromatic compounds of gas oil and is also remarkable, without decreasing the oil content by overcracking.

A serious issue concerning the cost and process of upgrading heavy oils arises from the deactivation of catalyst. Reactions involving the catalytic upgrading of heavy oils are likely to produce solid carbonaceous deposits, widely referred to as 'coke' (Dim et al., 2014). The deposition of coke on fresh catalyst results in the deactivation of the catalyst which reduces its useful life. The profitability of a catalytic process is dependent on the catalyst's lifetime hence these catalysts have to be regenerated before they can be used again (Hart, 2014). The characterization of coke on spent catalyst has become of very significant interest as catalyst deactivation has become a major concern in the refining industry (Daligauxet al., 2022). Catalyst deactivation occurs as a result of basically two reasons which are metal deposition and coke formation and deposition. Other causes of catalyst deactivation include poisoning, fouling, sintering as well as chemical and thermal degradation. Deactivation has been found out to be dependent on the nature of the feed and its composition, process parameters and reactor design. The rate of deactivation is also faster when the heavy oil that is to be upgraded has high content of asphaltenes and metals (Maity et al., 2012). Coking in catalytic upgrading of heavy oil presents a challenge in that it occurs in side reactions to the main reaction and, therefore, in contrast to poisoning, fouling and other causes of catalyst activation, which can be controlled and minimized by improving feed purification and better control of operating condition respectively, coking cannot be completely eliminated. Due to the industrial importance of the catalytic cracking of heavy oils, many articles have been published on the process and on the characterization of coke deposition on spent catalyst in order to understand the coking behavior, influence of process parameters and feed composition

on catalyst deactivation and to obtain relevant information on the structure and composition of coke formed and deposited during the catalytic upgrading of heavy oils.

This research work is aimed at thermally and structurally characterizing coke deposition on NiMo catalyst used in catalytic upgrading of heavy oil. The thermal characterization of coke was carried out using thermogravimetric analysis (TGA) to find out its thermal stability and the fraction of volatile components by monitoring the weight change that occurs as the coke sample was heated by gradually raising the temperature of a sample in a furnace as weight is measured at a constant rate (2.5, 5.0 and 15 °C/min respectively). Structural characterization was carried out using three methods which are Scanning Electron Microscopy (SEM), X-Ray Diffraction (XRD) and Fourier Transform Infrared (FTIR).

SEM is used to characterize the morphology of the formed-coke deposited at the outer layer of the catalyst pellet as well as the crystalline structure and orientation of materials making up the catalyst sample. X-ray diffraction is a technique that provides detailed information about the crystallographic structure and physical properties of materials. The physicochemical properties and microstructure of spent NiMo catalyst are characterized by X-ray diffraction to determine type of crystal and crystallinity of the spent catalyst. FTIR is carried out to ascertain the nature of the coke species that were extracted from the spent catalyst. It is used for characterizing the morphology of the sample and detecting the types of functional groups of the formed-coke on the sample. Characterizing coke deposition helps to identify the nature, location, structure and composition of coking material which is very essential for designing of improved and commercially viable catalysts.

## **2. MATERIAL AND METHODS**

### **Fresh Catalyst Properties**

The used catalyst studied in this work is a commercial sample of Ketjenfine hydro-processing catalyst Nickel-Molybdenum (NiMo) (Extrudates) from United States (US). The composition and properties of catalysts studied as specified are Precipitated silica: < 10; Nickel (II) oxide: < 10; Molybdenum (VI) oxide: < 30; Phosphorus pentoxide: 0-9; Aluminum oxide: balance (w/w%) of particles with diameter ~1mm and with a length of ~7mm, color is yellow, melting point is greater than 800°C, bulk density is 550 - 950 kg m<sup>-3</sup> and odorless. The spent catalyst is the reaction product of Canadian heavy oil in a Micro-reactor in presence of nitrogen gas at 425 °C, 20 bars for 8 hours.

### **2.1 The Fourier Transform Infrared Spectroscopy (FTIR)**

Fourier transform infrared spectroscopy (FT-IR) analysis was performed for all samples isolated to have a prompt result regarding the bio mineral. A few crystals were mixed with KBr (Merck for spectroscopy) and pulverized in an agate mortar to form a homogenous powder from which, under a pressure of 7 tons, the appropriate pellet was prepared. All spectra were recorded from 4000 to 400  $\text{cm}^{-1}$  using the Pelkin Elmer 3000 MX spectrometer. Scans were 32 per spectrum with a resolution of 4  $\text{cm}^{-1}$ . The IR spectra were analyzed using the spectroscopic software Win-IR Pro Version 3.0 with a peak sensitivity of 2  $\text{cm}^{-1}$ . The data was analyzed on computer system and the result presented in a graphical form.

## **2.2 Thermo-gravimetry Analysis (TGA)**

Thermo-gravimetric analysis (TGA) is an analytical technique where the weight of a sample is measured over time, as the temperature changes while heating. Typical weight loss profiles are analyzed to obtain the amount or percent of weight loss at any given temperature and the amount or percent of non-combusted residue at final temperature, and the temperature of various degradation steps. The analysis was carried out for each sample in a thermal gravimetric analyzer SDT Q600 V8.3. Gas flow and pressure were controlled by a pressure/flow controller. Time (min), weight (mg), heat flow (mW), temperature ( $^{\circ}\text{C}$ ) and temperature difference ( $^{\circ}\text{C}$ ) data were acquired at defined intervals and the data stored on the computer's hard disk. The analysis was carried out at 3 different heating rates (2.5, 5 and 15  $^{\circ}\text{C}/\text{min}$  respectively). The temperature range for heating was between 25 to 1005 ( $^{\circ}\text{C}$ ) for each sample and the flow rate of nitrogen used was 20.0 ml/min. Data from thermo-gravimetric analysis was analyzed on computer system and shown by a graph representing weight % as a function of temperature.

## **2.3 Scanning Electron Microscopy (SEM)**

All samples must be of an appropriate size to fit in the specimen chamber and are generally mounted rigidly on a specimen holder called a specimen stub. Several models of SEM can examine any part of a 6-inch (15 cm) semiconductor wafer, and some can tilt an object of that size to 45 $^{\circ}$ . Samples were coated with platinum coating of electrically conducting material, deposited on the sample either by low-vacuum sputter coating or by high-vacuum evaporation. SEM instruments place the specimen in a relative high-pressure chamber where the working distance is short and the electron optical column is differentially pumped to keep vacuum adequately low at the electron gun. The high-pressure region around the sample in the ESEM neutralizes charge and provides an amplification of the secondary electron signal. The SEM of the fresh

catalyst was carried out at 5, 10 and 20  $\mu\text{m}$  while that of the spent catalyst was carried out at 5, 20 and 50  $\mu\text{m}$ .

## 2.4 X-ray diffraction (XRD)

Powdered samples were pelletized and sieved to 0.074mm. These were later taken in an aluminum alloy grid (35mm x 50mm) on a flat glass plate and covered with a paper. Wearing hand gloves, the samples were compacted by gently pressing them with the hand. Each sample was run through the Rigaku D/Max-III C X-ray diffractometer developed by the Rigaku Int. Corp. Tokyo, Japan and set to produce diffractions at scanning rate of  $2^\circ/\text{min}$  in the  $2$  to  $50^\circ$  at room temperature with a CuK $\alpha$  (Copper K- $\alpha$ : an x-ray energy frequently used in x-ray lab scale equipment) radiation set at 40kV and 20mA. The diffraction data (d value and relative intensity) obtained was compared to that of the standard data of minerals from the mineral powder diffraction file, ICDD which contained and includes the standard data of more than 3000 minerals.

## 3. RESULT AND DISCUSSION

### 3.1 TGA

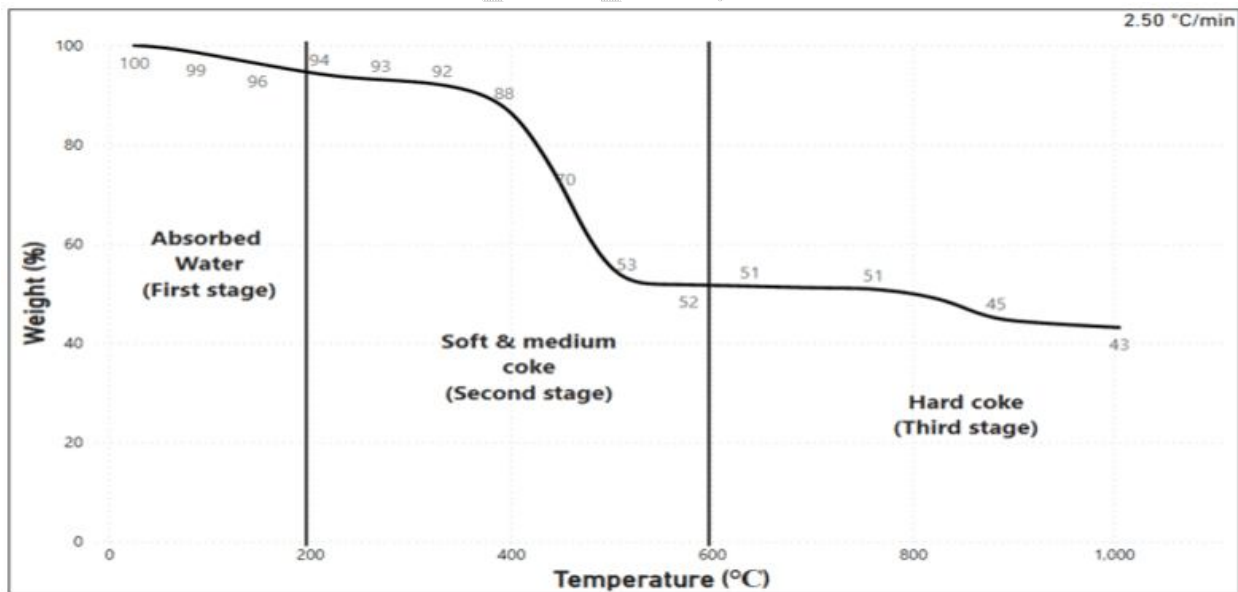


Figure 1. TGA profile of the spent NiMo catalyst at 2.50  $^\circ\text{C}/\text{min}$

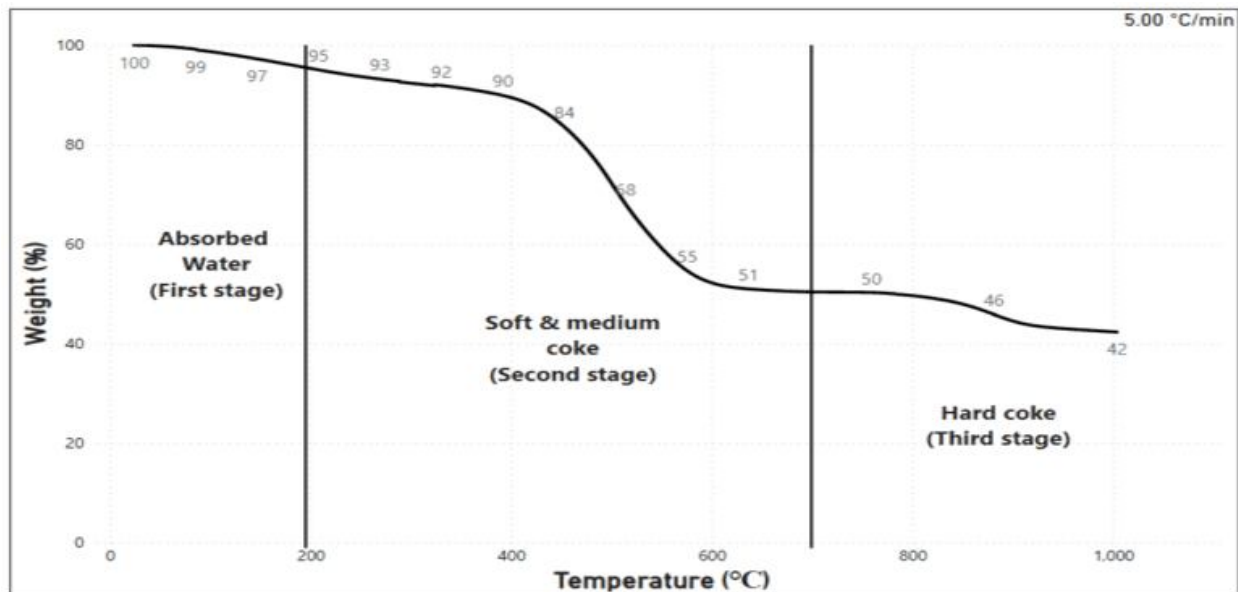


Figure 2. TGA profile of the spent NiMo catalyst at 5.00 °C/min

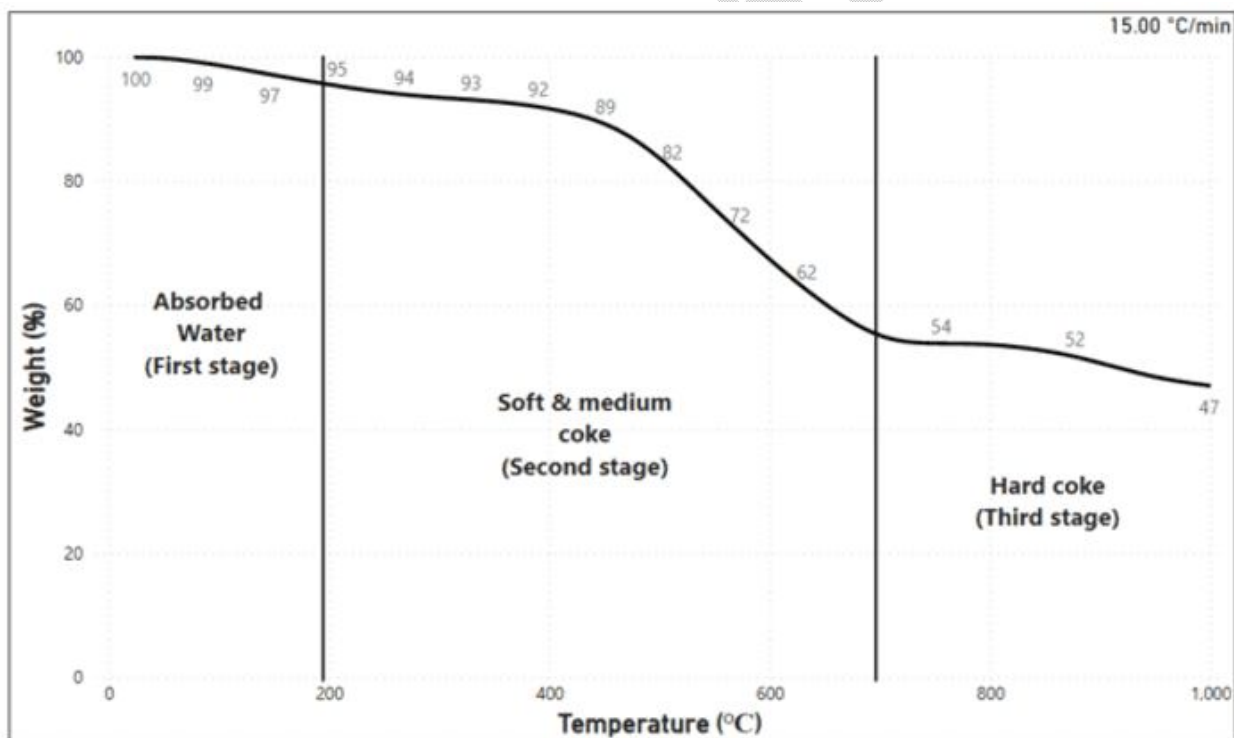
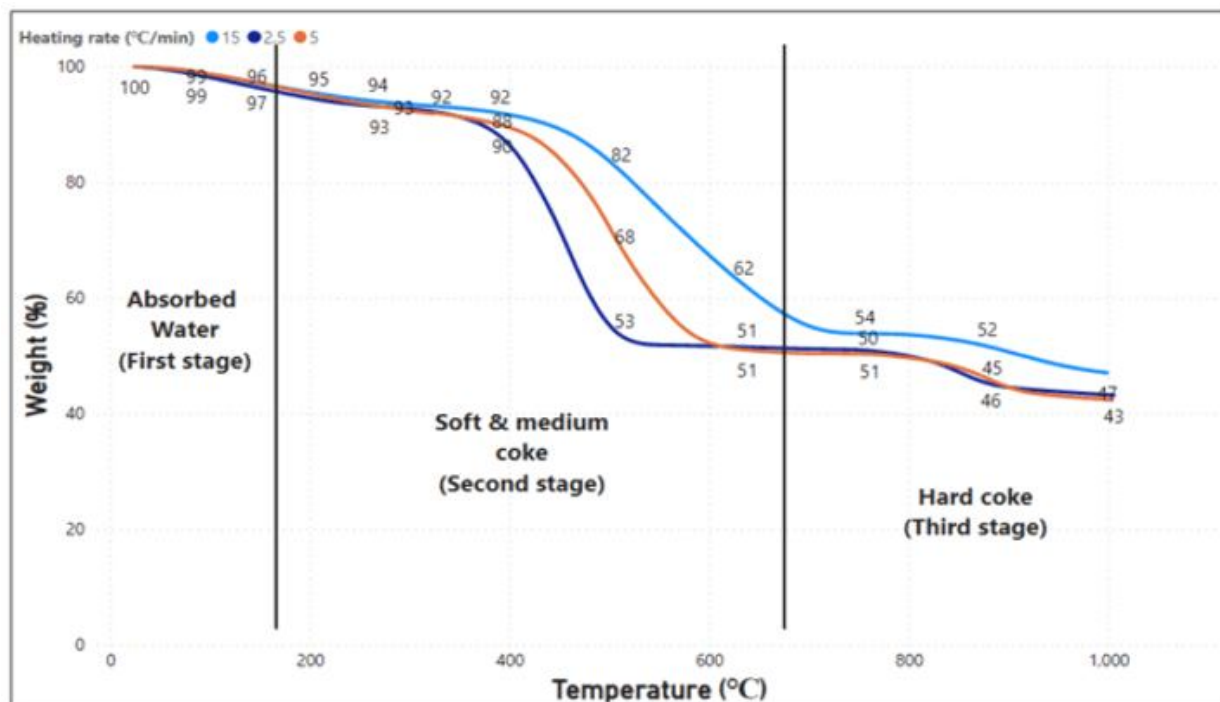


Figure 3. TGA profile of the spent NiMo catalyst at 15.00 °C/min



**Figure 4. TGA profile of the spent NiMo catalyst at 2.50, 5.00 and 15.00 °C/min (colored image\*)**

In this study, the total carbon deposited on the spent catalyst was investigated using TGA. Figures 1, 2 and 3 show the TGA graphs for heating rates of 2.50, 5.00 and 15.00 °C/min respectively and a constant Nitrogen flow rate of 20.0 ml/min while figure 4 is a TGA graph showing the weight losses of the 3 heating rates for comparison as well as the removal of volatile matter in the samples.

It was observed that as the temperature gradually increased for all samples, there was a continuous reduction in the weight of the spent catalyst. It was evident that the thermal decomposition of the samples had three different stages. TGA results indicated that the first weight loss in the range of 25-200°C signifies the presence of bonded water molecules and the dehydration of the moisture in the sample. It is also attributed to soft coke (light organic compounds present) desorption. The second weight loss stage occurred between 200-700°C and is attributed to the removal of soft and medium coke. The third weight loss stage occurred between 700-1005°C and is attributed to the removal of hard coke which decomposes slowly and is evident in the graphs.

Evidently, varying the heating rate (2.50 to 15.00 °C/min) did not affect the mass loss significantly. The total mass loss at 2.50 °C/min was about 57% whereas that at 15.00 °C/min was 53%. Generally, difference in mass loss could be due to the fact that more energy was added at the latter condition than at the beginning of the heating process.

### 3.2 X-ray Diffraction (XRD)

The X-ray Diffraction (XRD) measurements were performed on Catalyst powders using a diffractometer (BrukerAxS D8 Advance, Germany). CuK $\alpha$  radiation ( $\lambda = 1.54 \text{ \AA}$ ) was used at a voltage of 40 kV and a current of 25 mA.

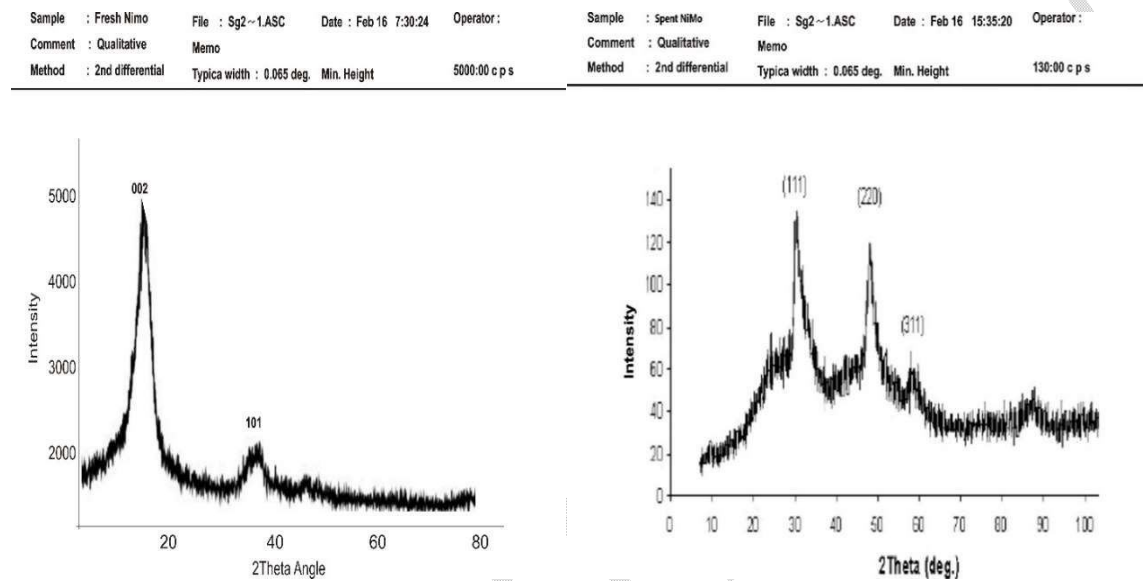


**Figure 5. XRD analysis of fresh NiMo** **Figure 6. XRD analysis of Spent NiMo**

The XRD of the prepared fresh and spent NiMo catalyst samples are shown in Figure 5 and 6 respectively. Fresh NiMo showed a major peak at  $36.7^\circ$  (hkl; 311) with a d-spacing 0.244 nm and a space group of  $227:Fd3m$ , while the other peaks observed at  $31.74^\circ$  and  $44.63^\circ$  with the corresponding planes of (220) and (400), respectively thus indicating the presence of a spinel phase of NiMo. A rutile phase with a tetragonal symmetry was detected for spent NiMo diffraction peaks, with the major phase (211) observed at  $54.32^\circ$  and a d-spacing of 0.16 nm. Diffraction peaks were observed at  $31.2^\circ$  and  $36.8^\circ$  with planes (220) and (311), respectively, with a space group of  $227:Fd3m$  of the cubic phase, thus indicating the presence of Carbon with a hexagonal phase with a major peak observed at  $32.8^\circ$  (hkl; 104) and a d-spacing of 0.27 nm.

### 3.3 FTIR Analysis

The FTIR analysis of the prepared fresh and spent NiMo catalyst samples are shown in Figure 7 and 8 respectively. The IR spectrum of calcinated fresh NiMo observed at  $912 \text{ cm}^{-1}$ , which corresponded to the stretching vibration of spent NiMo falling into inorganic bands and NiMo bonds, was indicative of the

crystal Fresh spinel [53 –55]. With spent NiMo, a peak identified at 900  $\text{cm}^{-1}$  corresponded to the vibration of NiMo, where the peak identified at 744  $\text{cm}^{-1}$  corresponded to O–C–O bond stretching vibrations depicting an anatase morphology because the band range of 500–800  $\text{cm}^{-1}$  followed the anatase crystal vibration modes. The presence of a small peak around 850  $\text{cm}^{-1}$  corresponded to O–C–O, which indicated the formation of CO. In the IR spectrum of CH, the small peak was slightly shifted below 700  $\text{cm}^{-1}$ , which could have been related to the stretching vibration of C–O bonding.

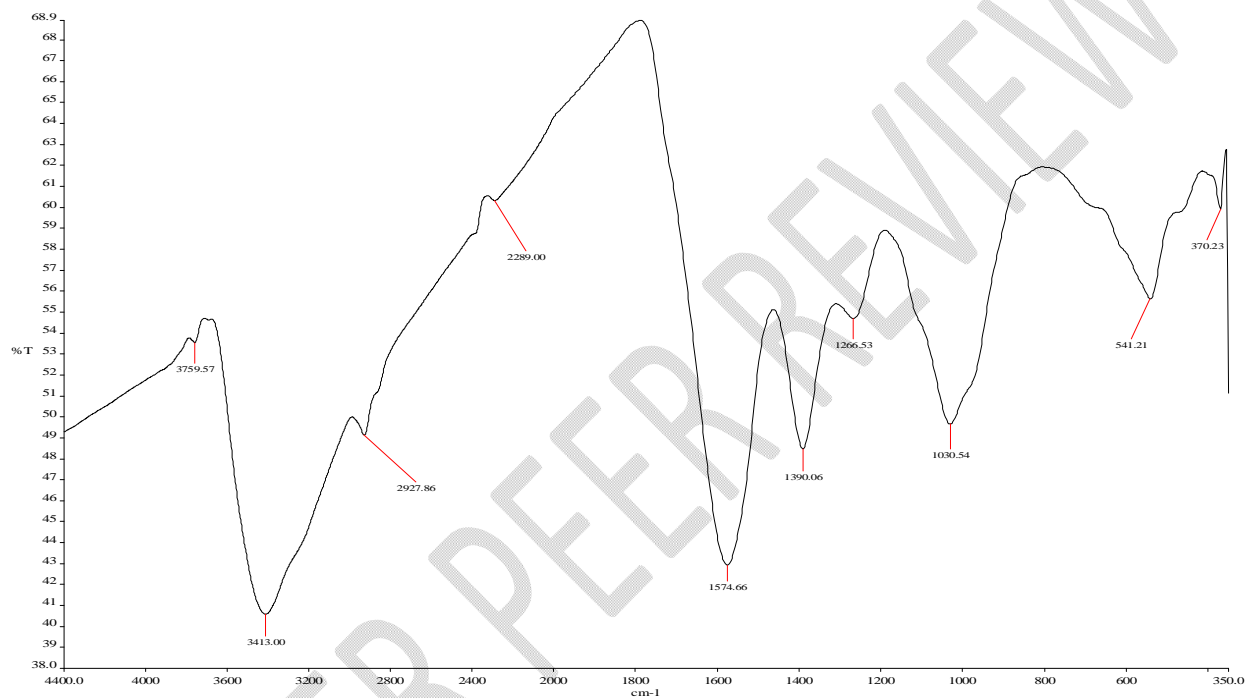


**Figure 7.** FTIR analysis of fresh NiMo catalyst

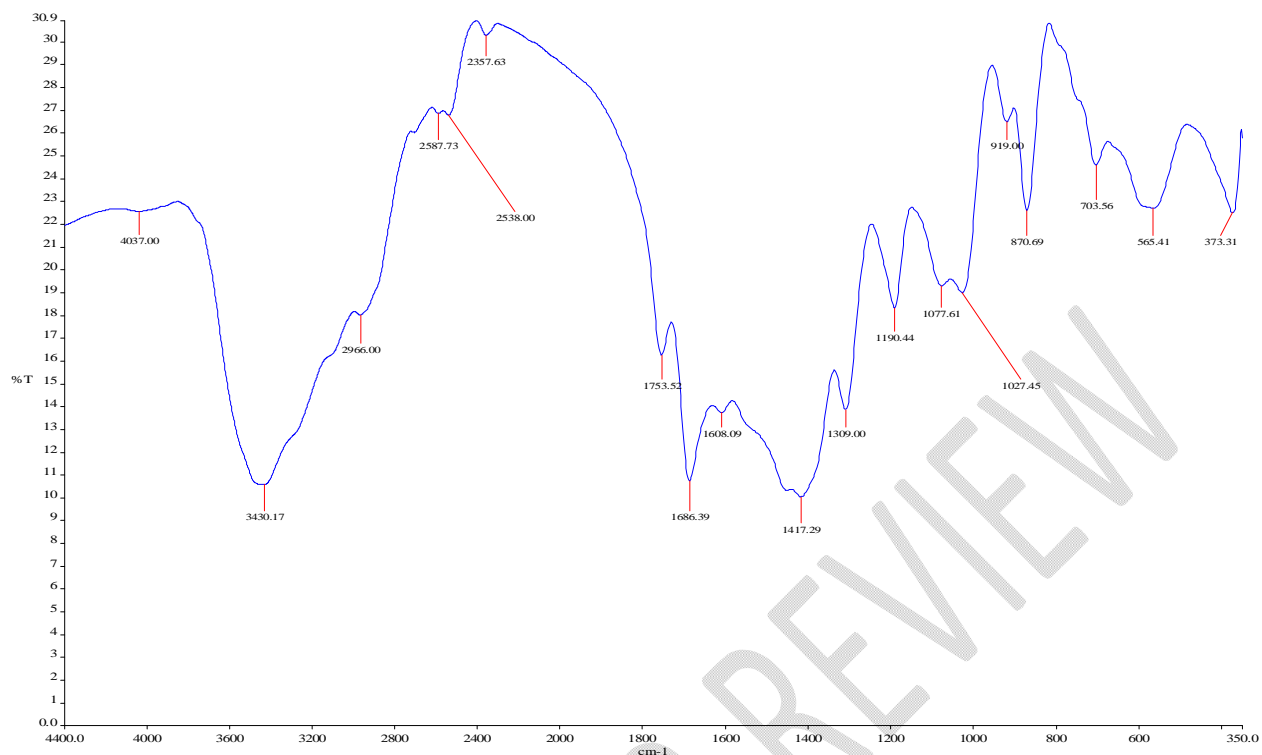


**Figure 8. FTIR analysis of spent NiMo catalyst**

### 3.4 SEM Analysis

Scanning electron microscopy analysis was used to investigate the morphology of the surface of the catalyst samples. The surface topography of the pure catalyst powder was characterized using Scanning Electron Microscopy (JSM-7600F JEOL, SEM, Japan) at an accelerating voltage of 20 kV and a working distance of 10 m.

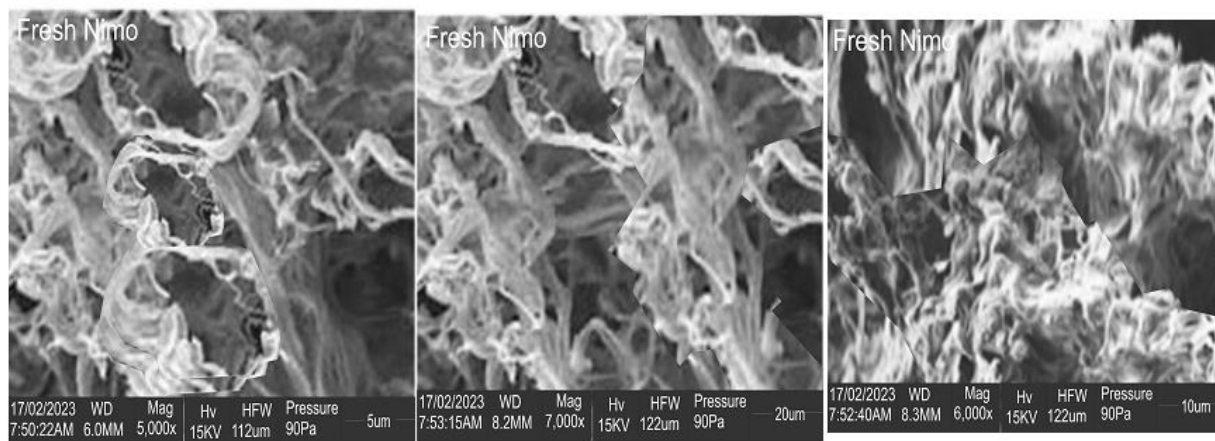


**Figure 9. SEM image of fresh NiMo catalyst**

The SEM micrograph of the fresh catalyst presented in Figure.9, shows the support surface that was modified after being exposed to the SEM. The carbon presence was confirmed by the elemental analysis, as shown in Figure 9 that indicates the presence of almost 4.5% carbon in the spent catalyst. Though different carbonaceous species were formed due to the reactive phase during the reaction, a carbon gasification at high temperature was expected and produced CO that had a higher syngas ratio. An SEM micrograph of NiMo particles is shown in Figure 9, which indicates the formation of porous-structure, block-shaped crystallites depicting the sintering of particles because of the higher temperature calcination.

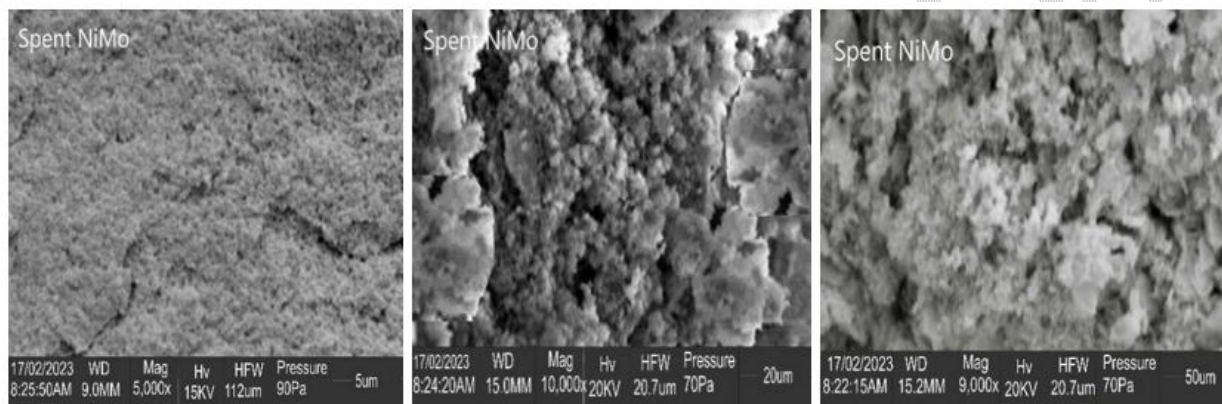


**Figure 10. SEM image of spent NiMo catalyst**

Sample was Ni- dominant whereas sample appeared to consist mainly of mixed-layer kaolin character with respect to the formamide test. Low magnification SEMs showed catalyst material with abundant pore space held together by a meshwork of clay coatings over relatively fresh NiMo (Fig..9). The NiMo itself was composed of a crinkled mass of flat, platy particles, often with curled edges, about 1-2  $\mu\text{m}$  diameter. There was abundant micro-pore space between the platy particles. The clay-rich nature of sample is evident from low magnification SEMs, the whole consisting of crinkled flakes and aggregates. The catalyst nature of sample is evident from low magnification SEMs, the whole consisting of crinkled flakes and aggregates arranged in sub- parallel fashion and with abundant void space. The constituent particles were mostly of an equant (in circles and having approximately equal diameters), platy shape, often bent or sinuous with curled edges, and ranged from  $\sim 0.5$  to 2  $\mu\text{m}$  diameter.

#### 4. CONCLUSION

The deposition of carbon on catalysts is the main cause of catalyst deactivation hence the study of the deactivation mechanism and the nature of carbonaceous deposits. This research work shows the thermal and structural characterization of fresh and Spent NiMo catalyst using TGA, XRD, FTIR and SEM. De-Coking process has been well described using TGA. TGA results indicated that the first weight loss in first heating stage signifies the presence of bonded water molecules while the 'medium' and 'hard' coke (second and third stage) are the most abundance species. The TGA analysis indicated a similar amount of carbon deposition and similar mass loss for the spent catalyst at the 3 different heating rates the analysis was carried out. The XRD characterization of the fresh and spent catalyst have shown presence of nickel and molybdenum species in a spinel phase. A rutile phase with a tetragonal symmetry was detected for spent NiMo diffraction peaks, with the major phase indicating the presence of Carbon with a hexagonal phase. The FTIR analysis of the spent NiMo shows a peak identified at  $900\text{ cm}^{-1}$  corresponded to the vibration of NiMo, while the peak identified at  $744\text{ cm}^{-1}$  corresponded to O–C–O bond stretching vibrations depicting an anatase morphology. The SEM micrograph of the fresh catalyst, shows the support surface. The carbon presence was confirmed by the elemental analysis is carried out and it indicates the presence of almost 4.5% carbon in the spent catalyst. An SEM micrograph of Nimo particles was visible which indicates the formation of porous-structure, block-shaped crystallites depicting the sintering of particles because of the higher temperature calcination.

## HIGHLIGHTS

- Experimental technique for coking of catalyst for optimization before characterization
- Methods to understand nature, position of coke and condition of spent catalyst
- Monitoring of decoking behavior to assess impact at different heating rates

## REFERENCE

- Argyle, M. D. and Bartholomew, C. H. (2015), "Heterogeneous catalyst deactivation and regeneration: A review", *Catalysts*, 5(1), 145-269, doi: 10.3390/catal5010145
- Asiedu, A., Davis, R. and Kumar, S. (2020), "Catalytic transfer hydrogenation and

characterization of flash hydrolyzed microalgae into hydrocarbon fuels production (jet fuel)”, *Fuel*, 261(2020), 116440, doi: 10.1016/j.fuel.2019.116440

Bare, S. R., Vila, F. D., Charochak, M. E., Prabhakar, S., Bradley, W. J., Jaye, C., Fischer, D. A. and Rehr, J. J. (2017), “Characterization of coke on a Pt-Re/ $\gamma$ -Al<sub>2</sub>O<sub>3</sub> re-forming catalyst: experimental and theoretical study”, *ACS Catalysis*, 7 (2), 1452-1461, doi: 10.1021/acscatal.6b02785

Charisiou, N. L., Douvartzides, S. L., Siakavelas, G. I., Tzounis, L., Sebastian, V., Stolojan, V., Hinder, S. J. and Goula, M. A. (2019), “The relationship between reaction temperature and carbon deposition on Nickel catalysts based on Al<sub>2</sub>O<sub>3</sub>, ZrO<sub>2</sub> or SiO<sub>2</sub> supports during the biogas dry reforming reaction”, *Catalysts*, 9(8), 676, doi: 10.3390/catal9080676

Chen, X., Ren, L., Yaseen, M., Wang, L., Liang, J., Liang, R. and Guo, H. (2019), “Synthesis, characterization and activity performance of Nickel-loaded spent FCC catalyst for pine gum hydrogenation”, *RSC Advances* 9(12), 6515-6525, doi: org/10.1039/C8RA07943A

Díaz, C. A., Garzón, W. F., Higuaita, J. C. and Restrepo-Parra, E. (2018), “Characterization by TGA, SEM, and EDX of polymeric matrices used as cocaine camouflages”, *Modern Applied Science* 12(12), 119, doi: 10.5539/mas.v12n12p119

Dim, P., Hart, A., Wood, J., Macnaughtan, B. and Rigby, B. S. (2015), “Characterization of pore coking in catalyst for thermal down-hole upgrading of heavy oil”, *Chemical Engineering Science*, 131(1), 138–145, doi: 10.1016/j.ces.2015.03.052

Dim, P., Rigby, S., Hart, A. and Wood, J. (2014), “Optimization of coke resistant catalyst for thermal down-hole upgrading”, *Chemical Engineering Science*, doi: org/10.2118/170070-

MS

- Dong C., Yin C., Wu T., Wu Z., Liu D. and Liu C. (2019), “Acid modification of the unsupported NiMo catalysts by Y-Zeolite nanoclusters”, *Crystals*, 9(7), 344, doi: 10.3390/cryst9070344
- Feng, R., Qiao, K., Wang, Y. and Yan, Z. (2013), “Perspective on FCC catalyst in China”, *Applied Petrochemical Research*, 3(3) 63–70, doi: 10.1007/s13203-013-0030-1
- Haridoss, S. (2017), “A study on role of catalyst used in catalytic cracking process in petroleum refining”, *International Journal of ChemTech Research*, 10(7), 79-86, doi: 10.1021/acs.energyfuels.2c00567
- Hart, A., Adam, M., Robinson, J.P., Rigby, S.P. and Wood, J. (2020), “Hydrogenation and dehydrogenation of Tetralin and Naphthalene to explore heavy oil upgrading using NiMo/Al<sub>2</sub>O<sub>3</sub> and CoMo/Al<sub>2</sub>O<sub>3</sub> catalysts heated with steel balls via induction”, *Catalysts*, 10(5), 497, doi: 10.3390/catal10050497
- Hart, A., Leeke, G., Greaves, M. and Wood, J. (2014), “Downhole Heavy Crude Oil Upgrading Using-CAPRI: Effect of Steam upon Upgrading and Coke Formation”, *Energy & Fuels*, 28(3), 1811-1819, doi: 10.1021/ef402300k
- Ihediwa, C. (2021), “Fluid catalytic cracking”, Kansa State University, retrieved from <https://hdl.handle.net/2097/41695>
- Leyva, C., Ancheyta, J., Mariey, L., Travert, A. and Mauge, F. (2014), “Characterization study of NiMo/SiO<sub>2</sub>-Al<sub>2</sub>O<sub>3</sub> spent hydroprocessing catalysts for heavy oils”, *Catalysis Today* 220–222, 89–96, doi: 10.1016/j.cattod.2013.10.007
- Modekwe H.U., Mamo M.A., Moothi K. and Daramola M.O (2021), “Effect of different catalyst

supports on the quality, yield and morphology of Carbon nanotubes produced from waste polypropylene plastics”, *Catalysts*, 11(6), 692, doi: 10.3390/catal11060692

Mortezaeikia, V., Tavakoli, O. and Khodaparasti, M. S. (2021), “A review on kinetic study approach for pyrolysis of plastic wastes using thermogravimetric analysis”, *Journal of Analytical and Applied Pyrolysis*, 160(1), 105340, doi: 10.1016/j.jaap.2021.105340

Nadeina, K. A., Budukva, S. V., Vatutina, Y. V., Mukhacheva, P. P., Gerasimov, E. Y., Pakharukova, V. P., limov, O. V. and Noskov, A. S (2022). “Unsupported Ni—Mo—W hydrotreating catalyst: influence of the atomic ratio of active metals on the HDS and HDN activity”, 12(12),1671, *Catalysts*, 12(2)1671, doi: 10.3390/catal12121671

Nagar, N., Garg, H. and Gahan, C.S. (2021), “Characterization of different types of petroleum refinery spent catalyst followed by microbial mediated leaching of metal values”, *Chem Rep*, 3(1),177-187, doi: 10.25082/CR.2021.01.002

Palos, R., Gutiérrez, A., Arandes, J. M. and Bilbao, J. (2018), “Catalyst used in fluid catalytic cracking (FCC) unit as a support of NiMo catalyst for light cycle oil hydroprocessing”, *Fuel*, 216 (2018), 142–152, doi: 10.1016/j.fuel.2017.11.1486

Silvarrey, L. S. and Phan, A. N. (2016), “Kinetic study of municipal plastic waste”, *International Journal of Hydrogen Energy*, 41(3), 16352-16364,doi: 10.1016/j.ijhydene.2016.05.202

Sundaram H. (2017), “A study on role of catalyst used in catalytic cracking process in petroleum refining”, *International Journal of ChemTech Research*, 10(7), 79-86

Trueba, D., Palos, R., Bilbao, J., Arandes, J. M. and Gutiérrez, A. (2021), “Product composition and coke deposition in the hydrocracking of polystyrene blended with vacuum gasoil”, *Fuel Processing Technology*, 224(2021) 107010, doi: 10.1016/j.fuproc.2021.107010

- Zahran, A. I., Ahmed M.A., Wael, A. A., Mohamed, A. S., Huda, S. A. and Mohamed, A. M. (2020), "Enhancement of heavy vacuum gas oil desulfurization via using developed catalyst based on Al<sub>2</sub>O<sub>3</sub>", *Egyptian Journal of Chemistry*, 63(10), 3801-3810, doi:10.21608/ejchem.2020.24452.2457
- Zhang, Y. S., Lu, X., Owen, R. E., Manos, G., Xu, R., Wang, F. R. and Brett, R. D. (2019), "Fine Structural changes of fluid catalytic catalysts and characterization of coke formed resulting from heavy oil devolatilization", *Applied Catalysis B: Environmental*, 263:118329, doi: 10.1016/j.apcatb.2019.118329
- Zhang, Y. S., Sun, G., Gao, S. and Xu, G. (2015), "Regeneration kinetics of Spent FCC catalyst via coke gasification in a micro fluidized bed", *Procedia Engineering*, 102(2015), 1758 – 1765, doi: 10.1016/j.proeng.2015.01.312